CrystEngComm

COMMUNICATION

View Article Online
View Journal | View Issue

Cite this: *CrystEngComm*, 2018, **20**, 2902

Received 2nd February 2018,
Accepted 13th April 2018

DOI: 10.1039/c8ce00171e

rsc.li/crystengcomm

Reentrant phase transformation from crystalline ikaite to amorphous calcium carbonate†

Zhaoyong Zou, Luca Bertinetti, Wouter J. E. M. Habraken and Peter Fratzl *

We report the spontaneous transformation of highly hydrated crystalline ikaite into less hydrated amorphous calcium carbonate (ACC), which has the outer contours of micrometer-sized crystals, a multi-level interconnected porous structure and a very high specific surface area (98.3 $cm^2\ g^{-1}$). The ikaite was previously obtained by transformation of an uncommon hydrated ACC with as much H_2O as ikaite, synthesized at 2 °C without any additives. The solid-state amorphization was induced by the fast dehydration of the crystal.

According to the well-known Ostwald rule,[1] thermodynamically less stable phases appearing first in a precipitate from solution further transform into more stable phases until the most stable crystalline phase is formed. In general, amorphous materials as the most unstable solid states would typically transform into more stable crystalline phases.[2,3] In the case of calcium carbonate, for example, amorphous calcium carbonate (ACC) has been widely observed as a transient precursor for the formation of crystalline calcium carbonate biominerals.[4] Here, we report that the opposite transformation from a crystalline calcium carbonate phase into ACC can also happen spontaneously.

Solid state amorphization, a process where a crystalline phase transforms into an amorphous state, may happen through a large input of energy necessary for such an energetically "uphill" conversion of structures. A typical example is mechanical grinding of crystalline materials, which may lead to amorphous materials *via* generation of localized heating followed by quenching, *via* an increase in disorder or massive creation of defects.[5,6] It can also be caused by hydrogenation of intermetallics where hydrogen atoms in crystalline phases are less energetically favourable.[7] In addition, dehydration of crystalline hydrates has been demonstrated as a route to the amorphous state of several organic solids[5] or copper sulphate pentahydrate.[8] Finally, crystalline coordination networks or highly porous metal–organic frameworks become amorphous upon losing constitutional solvent molecules.[9,10]

Ikaite is a highly hydrated crystalline calcium carbonate phase ($CaCO_3{\cdot}6H_2O$) containing discrete $CaCO_3$ ion pairs each surrounded by an envelope of 18 water molecules.[11] The neighbouring ion pairs are linked by hydrogen bonds only, which are temperature sensitive.[12] Therefore, ikaite is only stable at temperatures below 5 °C and in the natural environment it is only found in cold seawater, deep-sea sediment,

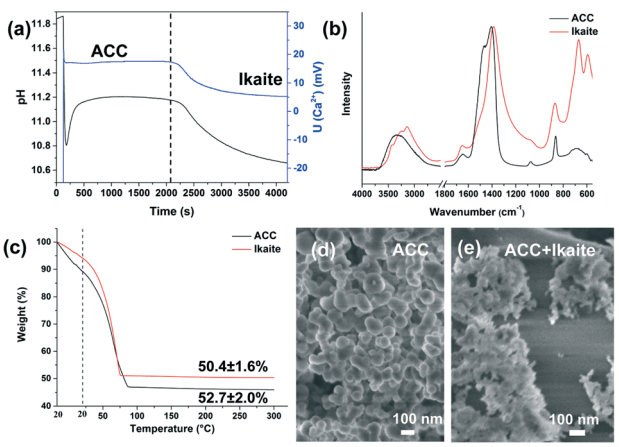

Fig. 1 (a) The evolution of pH and calcium activity (indicated by the measured potential from a calcium electrode) of the reaction solution. (b) The FTIR spectra of ACC and ikaite measured directly after filtration. (c) The TGA curves of ACC and ikaite where the temperature was maintained at 20 °C for 25 min before they were heated to 300 °C at a rate of 1.5 °C min^{-1}. The SEM images of ACC (d) and a sample during transformation (~2400 s, ACC + ikaite) (e).

Max Planck Institute of Colloids and Interfaces, Potsdam, 14476, Germany. E-mail: Peter.Fratzl@mpikg.mpg.de

† Electronic supplementary information (ESI) available: Detailed experimental procedures, characterization of the ikaite sample after filtration, TGA curves of different ACC samples, FTIR spectra of different ACC samples, morphology of the ACC transformed from ikaite and SAXS analysis of the sample under heating (PDF), and a video of the ACC investigated by FIB/SEM (mpg). See DOI: 10.1039/c8ce00171e

and cold spring water where the temperature is near 0 °C.[13,14] At elevated temperatures, it usually transforms into thermodynamically more stable calcite or vaterite, with the characteristic shape of ikaite preserved.[15,16] However, the mechanism that governs these transformation processes is not clear.

In this study, we aim at understanding the mechanisms for the unusual transformation of crystalline ikaite to ACC. We find that ikaite can first be obtained by the transformation of ACC with more than 6 H_2O per $CaCO_3$ in solution at 2 °C. More interestingly, we find that fast dehydration of this crystalline ikaite can induce its subsequent transformation into less hydrated ACC with a multi-level interconnected porous structure with a high specific surface area. Our findings show that a hydrated crystal can be converted into an amorphous solid just by sufficiently fast removal of water.

Using the procedure described in a previous study,[17] the formation of ACC and its transformation into ikaite are investigated by adding 0.5 mL 1 M $CaCl_2$ solution into 49.5 mL 20.2 mM Na_2CO_3 solution at 2 °C under stirring. *In situ* pH and calcium activity measurements (Fig. 1a) suggest that ACC precipitates immediately after the addition of $CaCl_2$ solution at 120 s and it remains stable in the mother solution for ~2000 s before it transforms into crystalline calcium carbonate with lower solubility.[17] Samples are collected at different stages of the reaction by vacuum filtration of the solution and washing with ethanol to remove the surface water. The infrared spectra of the samples (Fig. 1b) confirm that the initial precipitate is amorphous and show that the one after crystallization is pure ikaite, which is further confirmed by XRD and Raman analysis (Fig. S1†). The similar relative intensities of the peaks corresponding to the OH stretching at 3320 cm^{-1} and the H_2O bending at 1646 cm^{-1} for the as-synthesized ACC and ikaite suggest that both samples contain similar amounts of water. The water contents are determined by performing thermogravimetric analysis (TGA), where the sample is first maintained at 20 °C under a nitrogen flow (20 mL min^{-1}) for 25 min and then heated at a rate of 1.5 °C min^{-1}. As shown in Fig. 1c, both samples dehydrate quickly even at 20 °C, and the average weight loss after 300 °C is 52.7 ± 2.0% for the as-synthesized ACC and 50.4 ± 1.6% for ikaite, corresponding to a composition of $CaCO_3{\cdot}6.2H_2O$ and $CaCO_3{\cdot}5.6H_2O$, respectively. Within the experimental error, the water content of ikaite corresponds to the known value of 6 H_2O molecules per $CaCO_3$.[11] Interestingly, the water content of the as-synthesized ACC is of the same order, an unusually high value as compared to roughly one H_2O molecule per $CaCO_3$ for both biogenic and synthetic ACC according to previous studies.[18–22] It should be noted that if the as-synthesized ACC sample is further dried under vacuum, it contains only ~0.8 H_2O molecules per $CaCO_3$ (Fig. S2†). As a comparison, the ACC synthesized at room temperature often contains less than 2 H_2O molecules per $CaCO_3$ after filtration and ~1.1 H_2O molecules per $CaCO_3$ after further drying under vacuum. These results clearly demonstrate the high mobility of water in the structure of ACC where the majority of water can be easily removed at room temperature under vacuum.

To understand how ACC transforms into ikaite, the morphology of samples during transformation was investigated. The scanning electron microscopy (SEM) images show that the ACC nanoparticles (Fig. 1d) are spherical in shape with an average diameter of 69 ± 27 nm. For the sample taken during transformation (Fig. 1e), there are many nanoparticles less than 30 nm attaching onto the surface of large ikaite crystals. These nanoparticles are clearly much smaller than the ACC precursor, suggesting that the ACC precursor is only partially dissolved and decomposed into these smaller nanoparticles. Afterwards, these nanoparticles attach onto the surface of ikaite crystals and seem to transform into ikaite *via* local dissolution–recrystallization. This phenomenon is similar to the transformation process from ACC to vaterite and calcite in a pure system, as observed in a previous study.[17]

It is well known that ikaite is very unstable at room temperature and can easily transform into vaterite or calcite.[15,16] However, surprisingly, here we found that ikaite can easily transform into ACC in air with low humidity or under vacuum.

The transformation of ikaite in air was measured *in situ* by XRD (Fig. 2a), which shows that the intensity of the sharp Bragg diffraction peaks of ikaite gradually decreases with time and finally only two broad humps corresponding to ACC could be observed. The transformation under vacuum was investigated by infrared spectroscopy (Fig. 2b), which shows that the peak corresponding to the out-of-plane bending mode ν_2 of the carbonate group shifts from 872 cm^{-1} to 862 cm^{-1} and becomes sharper, while the in-plane bending mode ν_4 of the carbonate group at 671 cm^{-1} shifts to a higher wavenumber at 694 cm^{-1} and becomes broader, confirming the transformation from ikaite to ACC without any other crystalline phases. Interestingly, while the asymmetric stretching mode ν_3 of the carbonate group gradually evolves into a shape corresponding to ACC with two splitting peaks, the position of the main peak remains at 1392 cm^{-1}, which is significantly lower than the typical values for both synthetic (Fig. S3†) and biogenic ACC samples (between 1406 and 1417 cm^{-1}).[17,18] This suggests that the local atomic structure of this ACC is different from the ACC formed from solution.

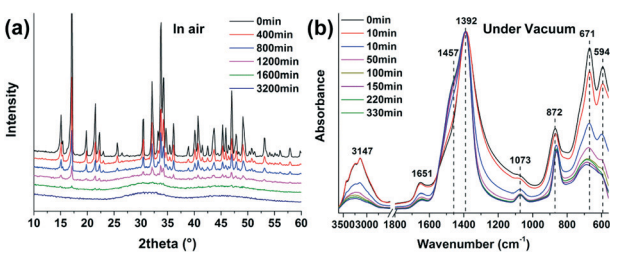

Fig. 2 (a) XRD patterns of the ikaite measured *in situ* in air at room temperature. (b) FTIR spectra of the ikaite stored under vacuum.

Since ikaite has 6 H_2O per $CaCO_3$ and the ACC obtained from ikaite transformation under vacuum has only 0.6 H_2O per $CaCO_3$, ~90% of the water is expelled out of the crystal. Using the densities of ikaite (1.82 g cm^{-3})[23] and ACC (2.43 g cm^{-3}),[24] the volume fraction corresponding to the loss of water should be ~58%. However, the SEM image (Fig. 3c) of ACC shows that the external shape of ikaite crystals is preserved, but there are many cracks on the surface, suggesting that ACC is highly porous. To understand the transformation process, the nanostructure of ACC was further investigated by focused ion beam/scanning electron microscopy (FIB/SEM). Interestingly, results show that ACC is composed of a huge amount of pores and channels hundreds of nanometers in size (Fig. 3d and S4 and Video S1†), which are interconnected and also connected to the cracks observed on the surface. However, the volume fraction of the pores and channels estimated from the analysis of the image stacks is only ~26%, suggesting the existence of even smaller pores. To investigate this further, the sample was also measured by nitrogen adsorption and the data were analysed with the Brunauer–Emmett–Teller (BET) method (Fig. 3a and b). The analysis shows an isotherm with a high sorption capacity at a relative pressure (P/P_0) of ~0.5, revealing the presence of abundant mesopores, which are characterized by a specific surface area of 98.3 m^2 g^{-1} and an average pore diameter of 3.96 nm. The cumulative pore volume is 0.10 cm^3 g^{-1}, corresponding to a volume fraction of ~24%. Thus, the volume fraction of all the pores is ~50%, which fits quite well to the theoretical value by assuming that all these pores are caused by the loss of water during transformation.

To describe the dynamics of dehydration and phase transformation of ikaite under heating, TGA/DSC and *in situ* SAXS and WAXS analyses were performed at a heating rate of 3 °C min^{-1}. To avoid water-induced crystallization of calcite or vaterite on the surface of ikaite crystals, the N_2 flow was set

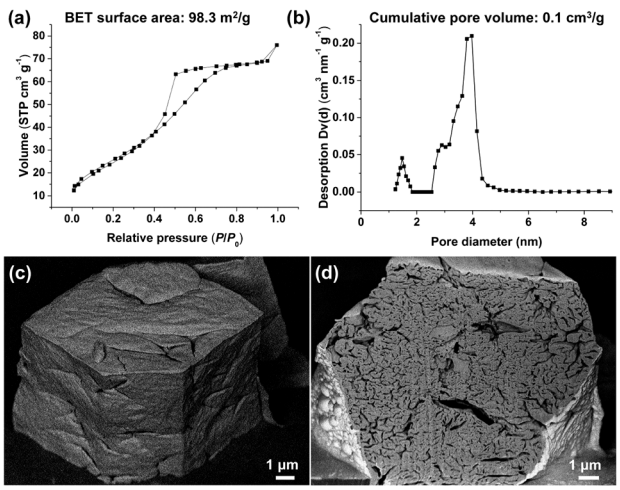

Fig. 3 N_2 adsorption/desorption isotherms at 77 K (a) and the corresponding differential pore volume distribution (Dv(d)) plot (b) of an ACC sample transformed from ikaite under vacuum. Backscattered SEM images showing the surface of ACC (c) and its cross-section after FIB milling (d).

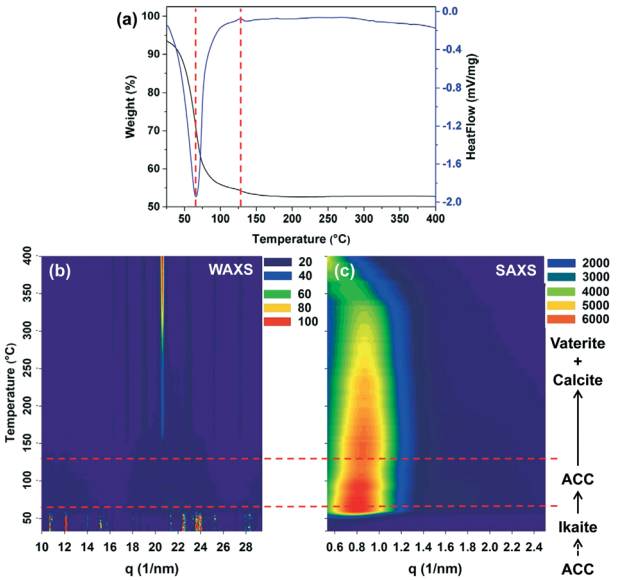

Fig. 4 TGA/DSC curves of the ikaite sample under heating at 3 °C min^{-1} (a) and the corresponding WAXS (b) and SAXS (Kratky plot, $I \times q^2$ *vs.* q) (c) patterns. The solid arrows on the right indicate the phase transformation during heating and the dashed arrow indicates that ikaite is transformed from ACC in solution. Note that the slight differences in the decomposition temperature from the TGA/DSC and WAXS/SAXS data could be due to the different heating set-ups and the rate of the N_2 flow.

at 200 ml min^{-1} for TGA/DSC measurement and 1 L min^{-1} for WAXS/SAXS analysis to remove water as fast as possible. The TGA/DSC curves (Fig. 4a) show a strong endothermic peak at 65 °C with more than 80% total weight loss, which is followed by an exothermic peak at 127 °C and a second stage of weight loss. Correspondingly, the WAXS patterns (Fig. 4b) show that the crystal structure of ikaite is maintained until being heated to ~55 °C, and then ikaite quickly transforms into ACC. ACC remains stable until ~130 °C and gradually transforms into a mixture of calcite and vaterite, instead of only calcite, as observed in previous studies.[17,25] After 350 °C, the intensity of the vaterite peaks slightly decreases, suggesting that vaterite further transforms into calcite. Correspondingly, a strong SAXS signal with a sharp peak at q = 0.8 nm^{-1} (7.8 nm in real space) and a broad hump at q = 2.0 nm^{-1} (3.1 nm in real space) appears after the decomposition of ikaite (Fig. 4c and S5a†). The intensity of the two peaks further increases upon increasing the temperature to 75 °C, while the sample remains amorphous, suggesting the formation of additional pores. During the crystallization of ACC into vaterite and calcite, the intensity of both peaks decreases very quickly. In addition, according to the linear fitting of the Porod plot (Fig. S5b†), the internal surface area increases quickly during the decomposition of ikaite and then slowly decreases during further crystallization of ACC.

Based on the above analysis, a clear picture of how ikaite transforms into ACC can be deduced. It is known that crystalline ikaite consists of discrete $CaCO_3$ ion pairs separated by water molecules and these ion pairs are joined by hydrogen

bonds only, which are the only forces enabling ikaite to maintain its crystallinity.[13,26,27] As ikaite dehydrates spontaneously at room temperature,[28] the rapid removal of water molecules results in the breakdown of hydrogen bonds, and the crystalline structure collapses to form an amorphous solid because the separated $CaCO_3$ units cannot easily rearrange themselves into a more stable crystalline phase in the solid-state. While such behaviour is known for metal–organic frameworks,[9,10] it is interesting to see that it may also occur for simple ionic compounds. However, if the dehydration process is not fast enough, heterogeneous nucleation of calcite or vaterite occurs. Previous studies have shown that moisture on the surface of ikaite accelerates its transformation to calcite at cool temperature (13 °C) and rapid transformation to vaterite is favoured at room temperature.[13] This suggests that kinetic factors such as temperature and the presence of water are critical in controlling the phase transformation of ikaite. Therefore, when ikaite crystals are washed with ethanol and exposed to air with low humidity, water adsorption on the surface is significantly inhibited and heterogeneous nucleation of calcite or vaterite is prevented. Recently, Dieckmann *et al.*[29] accidentally found the decomposition of ikaite crystals into ACC when they mistakenly stored the crystals in absolute ethanol (>99.9%), rather than in 50% ethanol. Apparently, this is also because of the rapid dehydration of ikaite in pure ethanol. Therefore, our results demonstrate that the rapid dehydration of ikaite promotes its transformation into ACC and the formation of nanocavities within the solid while the crystal shape of ikaite is preserved. This is very interesting because ACC usually forms spherical particles, whereby here we show that such a solid-state amorphization process can produce ACC resembling the precursor ikaite particles and may be used in the future to control the size and morphology of ACC deposits.

To summarize, here we discovered that ACC with ~6.2 H_2O per $CaCO_3$ can be synthesized at 2 °C and it transforms into ikaite *via* a partial dissolution–recrystallization process. More importantly, we found that ikaite can easily transform into ACC when the dehydration kinetics is fast enough to prevent the nucleation of more stable crystalline phases. Our study also provides another possibility for the transformation of ikaite to glendonite, where ikaite first decomposes into ACC and this metastable short-lived intermediate acts as the precursor for the formation of calcite. Moreover, the obtained ACC has a very high specific surface area and a multi-level porous structure, which could have many potential applications such as in drug delivery,[30] wastewater treatment,[31] *etc.*

Conflicts of interest

There are no conflicts to declare.

Acknowledgements

This research was supported by a German Research Foundation grant within the framework of the Deutsch–Israelische Projektkooperation DIP. Zhaoyong Zou was supported by the China Scholarship Council (CSC). Open Access funding provided by the Max Planck Society.

References

1 W. Ostwald, *Z. Phys. Chem.*, 1897, **22**, 289–330.
2 N. D. Loh, S. Sen, M. Bosman, S. F. Tan, J. Zhong, C. A. Nijhuis, P. Král, P. Matsudaira and U. Mirsaidov, *Nat. Chem.*, 2016, **9**, 77–82.
3 W. J. E. M. Habraken, J. Tao, L. J. Brylka, H. Friedrich, L. Bertinetti, A. S. Schenk, A. Verch, V. Dmitrovic, P. H. H. Bomans, P. M. Frederik, J. Laven, P. van der Schoot, B. Aichmayer, G. de With, J. J. DeYoreo and N. A. J. M. Sommerdijk, *Nat. Commun.*, 2013, **4**, 1507.
4 S. Weiner and L. Addadi, *Annu. Rev. Mater. Res.*, 2011, **41**, 21–40.
5 T. Einfalt, O. Planinšek and K. Hrovat, *Journal*, 2013, **63**, 305.
6 J. F. Willart and M. Descamps, *Mol. Pharmaceutics*, 2008, **5**, 905–920.
7 K. Aoki and T. Masumoto, *J. Alloys Compd.*, 1995, **231**, 20–28.
8 G. A. Specken and K. J. McCallum, *Nature*, 1960, **185**, 758.
9 K. Ohara, J. Martí-Rujas, T. Haneda, M. Kawano, D. Hashizume, F. Izumi and M. Fujita, *J. Am. Chem. Soc.*, 2009, **131**, 3860–3861.
10 S. Kitagawa, R. Kitaura and S. i. Noro, *Angew. Chem., Int. Ed.*, 2004, **43**, 2334–2375.
11 B. Dickens and W. E. Brown, *Inorg. Chem.*, 1970, **9**, 480–486.
12 I. P. Swainson and R. P. Hammond, *Mineral. Mag.*, 2003, **67**, 555–562.
13 T. Ito, *Geochem. J.*, 1998, **32**, 267–273.
14 G. S. Dieckmann, G. Nehrke, S. Papadimitriou, J. Göttlicher, R. Steininger, H. Kennedy, D. Wolf-Gladrow and D. N. Thomas, *Geophys. Res. Lett.*, 2008, **35**, L08501.
15 C. C. Tang, S. P. Thompson, J. E. Parker, A. R. Lennie, F. Azough and K. Kato, *J. Appl. Crystallogr.*, 2009, **42**, 225–233.
16 A. Zaoui and W. Sekkal, *Geoderma*, 2014, **235–236**, 329–333.
17 Z. Zou, L. Bertinetti, Y. Politi, A. C. S. Jensen, S. Weiner, L. Addadi, P. Fratzl and W. J. E. M. Habraken, *Chem. Mater.*, 2015, **27**, 4237–4246.
18 S. Weiner, Y. Levi-Kalisman, S. Raz and L. Addadi, *Connect. Tissue Res.*, 2003, **44**, 214–218.
19 Y. Politi, R. A. Metzler, M. Abrecht, B. Gilbert, F. H. Wilt, I. Sagi, L. Addadi, S. Weiner and P. U. P. A. Gilbert, *Proc. Natl. Acad. Sci. U. S. A.*, 2008, **105**, 17362–17366.
20 H. Nebel, M. Neumann, C. Mayer and M. Epple, *Inorg. Chem.*, 2008, **47**, 7874–7879.
21 A. V. Radha, T. Z. Forbes, C. E. Killian, P. U. P. A. Gilbert and A. Navrotsky, *Proc. Natl. Acad. Sci. U. S. A.*, 2010, **107**, 16438–16443.
22 M. P. Schmidt, A. J. Ilott, B. L. Phillips and R. J. Reeder, *Cryst. Growth Des.*, 2014, **14**, 938–951.

23 T. C. Council and P. C. Bennett, *Geology*, 1993, **21**, 971–974.
24 A. L. Goodwin, F. M. Michel, B. L. Phillips, D. A. Keen, M. T. Dove and R. J. Reeder, *Chem. Mater.*, 2010, **22**, 3197–3205.
25 J. Ihli, W. C. Wong, E. H. Noel, Y.-Y. Kim, A. N. Kulak, H. K. Christenson, M. J. Duer and F. C. Meldrum, *Nat. Commun.*, 2014, **5**, 3169.
26 A. R. Lennie, C. C. Tang and S. P. Thompson, *Mineral. Mag.*, 2004, **68**, 135–146.
27 G. Marland, *Geochim. Cosmochim. Acta*, 1975, **39**, 83–91.
28 A. Mikkelsen, A. B. Andersen, S. B. Engelsen, H. C. B. Hansen, O. Larsen and L. H. Skibsted, *J. Agric. Food Chem.*, 1999, **47**, 911–917.
29 G. S. Dieckmann, G. Nehrke, C. Uhlig, J. Göttlicher, S. Gerland, M. A. Granskog and D. N. Thomas, *Cryosphere*, 2010, **4**, 227–230.
30 W. Wei, G.-H. Ma, G. Hu, D. Yu, T. McLeish, Z.-G. Su and Z.-Y. Shen, *J. Am. Chem. Soc.*, 2008, **130**, 15808–15810.
31 E. Hautala, J. Randall, A. Goodban and A. Waiss, *Water Res.*, 1977, **11**, 243–245.